Light-Nuclei Spectra from Chiral Dynamics

M. Piarulli, A. Baroni, L. Girlanda, A. Kievsky, A. Lovato, Ewing Lusk, L. E. Marcucci, Steven C. Pieper, R. Schiavilla, M. Viviani, and R. B. Wiringa

Phys. Rev. Lett. **120**, 052503 — Published 1 February 2018

DOI: 10.1103/PhysRevLett.120.052503

Light-nuclei spectra from chiral dynamics

M. Piarulli[a], A. Baroni[b], L. Girlanda[c,d], A. Kievsky[e], A. Lovato[a,f], Ewing Lusk[g], L.E. Marcucci[e,h], Steven C. Pieper[a], R. Schiavilla[b,i], M. Viviani[e], and R.B. Wiringa[a]

[a] *Physics Division, Argonne National Laboratory, Argonne, Illinois 60439, USA*
[b] *Department of Physics, Old Dominion University, Norfolk, Virginia 23529, USA*
[c] *Department of Mathematics and Physics, University of Salento, 73100 Lecce, Italy*
[d] *INFN-Lecce, 73100 Lecce, Italy*
[e] *INFN-Pisa, 56127 Pisa, Italy*
[f] *INFN-Trento, 38050 Povo, Italy*
[g] *Mathematics and Computer Science Division, Argonne National Laboratory, Argonne, Illinois 60439, USA*
[h] *Department of Physics, University of Pisa, 56127 Pisa, Italy*
[i] *Theory Center, Jefferson Lab, Newport News, Virginia 23606, USA*

(Dated: December 6, 2017)

In recent years local chiral interactions have been derived and implemented in quantum Monte Carlo methods in order to test to what extent the chiral effective field theory framework impacts our knowledge of few- and many-body systems. In this paper, we present Green's function Monte Carlo calculations of light nuclei based on the family of local two-body interactions presented by our group in a previous paper in conjunction with chiral three-body interactions fitted to bound- and scattering-state observables in the three-nucleon sector. These interactions include Δ intermediate states in their two-pion-exchange components. We obtain predictions for the energy levels and level ordering of nuclei in the mass range $A = 4$–12, accurate to $\leq 2\%$ of the binding energy, in very satisfactory agreement with experimental data.

PACS numbers: 21.30.-x, 21.60.De,27.10.+h,27.20.+n

A major goal of nuclear theory is to explain the spectra, structure, and reactions of nuclei in a fully microscopic approach. In such an approach, which we will refer to below as the *basic model* of nuclear theory, the nucleons interact with each other via many-body (primarily, two- and three-body) effective interactions, and with external electroweak probes via effective currents describing the coupling of these probes to individual nucleons and many-body clusters of them.

The nuclear Hamiltonian in the basic model is taken to consist of non-relativistic kinetic energy, and two- and three-body interactions. There are indications that four-body interactions may contribute at the level of ~ 100 keV in ^{4}He, but current formulations of the basic model do not typically include them (see, for example, Ref. [1]). Two-body interactions consist of a long-range component, for inter-nucleon separation $r \gtrsim 2$ fm, due to one-pion exchange (OPE) [2], and intermediate- and short-range components, for, respectively, 1 fm $\lesssim r \lesssim 2$ fm and $r \lesssim 1$ fm. Up to the mid-1990's, such interactions were based almost exclusively on meson-exchange phenomenology. Those of the mid-1990's [3–5] were constrained by fitting nucleon-nucleon (NN) elastic scattering data up to lab energies of 350 MeV, with χ^2/datum $\simeq 1$ relative to the database available at the time [6]. Two well-known and still widely used examples in this class are the Argonne v_{18} (AV18) [4] and CD-Bonn [5]. These so-called *realistic* interactions also contained isospin-symmetry-breaking (ISB) terms. At the level of accuracy required [6], full electromagnetic interactions, along with strong interactions, had to be specified in order to fit the data precisely, and the AV18 model included electromagnetic corrections up to order α^2 (α is the fine structure constant).

Already in the 1980's, accurate three-body calculations showed that contemporary NN interactions did not provide enough binding for the three-body nuclei, ^{3}H and ^{3}He [7]. In the late 1990's and early 2000's this realization was extended to the spectra (ground and low-lying excited states) of light p-shell nuclei in calculations based on quantum Monte Carlo (QMC) methods [8] and later confirmed independently in no-core shell-model studies [9]. Consequently, the basic model with NN interactions fit to scattering data, without the inclusion of a three-nucleon ($3N$) interaction, is incomplete.

Because of the composite nature of the nucleon and, in particular, the prominent role of the Δ resonance in pion-nucleon scattering, multi-nucleon interactions arise quite naturally in meson-exchange phenomenology. The Illinois $3N$ interactions [10] contain a dominant two-pion exchange (TPE)—the venerable Fujita-Miyazawa interaction [11]—and smaller multi-pion exchange components resulting from the excitation of intermediate Δ's. The most recent version, Illinois-7 (IL7) [12], also contains phenomenological isospin-dependent central terms. The small number (four) of parameters that fully characterize it were determined, in conjunction with the AV18, by fitting 23 ground or low-lying nuclear states in the mass range A=3–10. The resulting AV18+IL7 Hamiltonian then led to predictions of about 100 ground- and excited-state energies up to A=12, including the ^{12}C ground- and Hoyle-state energies, in good agreement with the corre-

sponding empirical values [1].

A new phase in the evolution of the basic model, and renewed interest in its further development, have been spurred by the emergence in the early 1990's of chiral effective field theory (χEFT) [13–15], a low-energy effective representation of QCD. Within χEFT many studies have been carried out dealing with the construction of NN and $3N$ interactions [16–30] and accompanying ISB corrections [31–33]. These interactions were typically formulated in momentum space, and included cutoff functions to regularize their behavior at large momenta which, however, made them strongly non-local when Fourier-transformed in configuration space, and therefore unsuitable for use with quantum Monte Carlo methods. Among these, in particular, Green's Function Monte Carlo (GFMC) is the method of choice to provide reliable solutions of the many-body Schrödinger equation—presently for up to $A=12$ nucleons—with full account of the complexity of the many-body, spin- and isospin-dependent correlations induced by nuclear interactions (see Ref. [1] and references therein for an exhaustive review of GFMC).

In order to overcome these difficulties, in recent years local, configuration-space chiral NN interactions have been derived [34–36]. Here, we focus on the family of local interactions constructed by our group [36]. They are written as the sum of an electromagnetic-interaction component, $v_{ij}^{\rm EM}$, including first- and second-order Coulomb, Darwin-Foldy, vacuum polarization, and magnetic moment terms (as in Ref. [4]), and a strong-interaction component, v_{ij}, characterized by long- and short-range parts [36]. The long-range part includes OPE and TPE terms up to next-to-next-to-leading order (N2LO) in the chiral expansion [37], derived in the static limit from leading and sub-leading πN and $\pi N\Delta$ chiral Lagrangians. The short-range part is described by charge-independent contact interactions up to N3LO and charge-dependent ones up to NLO [36], characterized by a total of 26 low-energy constants (LECs). Such potentials should therefore be understood as *improved*-N2LO, with N3LO contact terms treated as phenomenological remainders that prove crucial for a good fit to NN data. In this context, it is worthwhile pointing out that there exist alternative counting schemes for contact operators [38–41] based, *e.g.*, on renormalization group analyses, that imply their promotion to lower orders of the low-energy expansion, as compared to the ordinary Weinberg counting. This would in turn explain the prominent role they take in bringing the theoretical description close to experimental data.

We constructed two classes of interactions, which only differ in the range of laboratory energy over which the fits were carried out, either 0–125 MeV in class I or 0–200 MeV in class II (the fits used the 2013 NN database, including the deuteron ground-state energy and two-neutron scattering length, as assembled by the Granada group [42]). For each class, three different sets of cutoff radii $(R_{\rm S}, R_{\rm L})$ were considered $(R_{\rm S}, R_{\rm L}) = (0.8, 1.2)$ fm in set a, (0.7,1.0) fm in set b, and (0.6,0.8) fm in set c, where $R_{\rm S}$ and $R_{\rm L}$ enter respectively the configuration-space cutoffs for the short- and long-range parts of v_{ij} [36]. The χ^2/datum achieved by the fits in class I (II) was $\lesssim 1.1 (\lesssim 1.4)$ for a total of about 2700 (3700) data points. We will refer to these high-quality NN interactions generically as the Norfolk v_{ij}'s (NV2s), and designate those in class I as NV2-Ia, NV2-Ib, and NV2-Ic, and those in class II as NV2-IIa, NV2-IIb, and NV2-IIc.

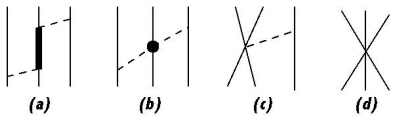

FIG. 1. Diagrams illustrating schematically the contributions to the chiral $3N$ interaction. Nucleons, Δ's, and pions are denoted by solid, thick-solid, and dashed lines, respectively. The circle in panel (b) represents the vertex involving the LECs c_1, c_3, and c_4 in $\mathcal{L}_{\pi N}^{(2)}$.

The NV2s were found to provide insufficient attraction, in GFMC calculations, for the ground-state energies of nuclei with $A=3$–6 [36, 43, 44], thus corroborating the insight realized in the early 2000's within the older (and less fundamental) meson-exchange phenomenology. To remedy this shortcoming, we construct here the leading $3N$ interaction V_{ijk} in χEFT, including Δ intermediate states. It is illustrated diagrammatically in Fig. 1, and consists [20, 21] of a long-range piece mediated by TPE and denoted with the superscript 2π, panels (a) and (b), and a short-range piece parametrized in terms of two contact interactions and denoted with the superscript CT, panels (c) and (d),

$$V_{ijk} = \sum_{\rm cyclic\ } \big(V_{ijk}^{2\pi} + V_{ijk}^{\rm CT} \big) \ . \qquad (1)$$

In configuration space, the TPE term from intermediate Δ states, panel (a) in Fig. 1, and from interactions proportional to the LECs c_1, c_3, and c_4 in the sub-leading chiral Lagrangian $\mathcal{L}_{\pi N}^{(2)}$ [45], panel (b), reads

$$V_{ijk}^{2\pi} = \frac{g_A^2}{256\,\pi^2}\frac{m_\pi^6}{f_\pi^4}\Big[8\,c_1\,\Sigma_{ij}\,\Sigma_{kj}\,\mathcal{T}_{ijk}^{(+)} + \frac{2}{9}\,\widetilde{c}_3\,\Sigma_{ijk}^{(+)}\,\mathcal{T}_{ijk}^{(+)} - \frac{1}{9}\Big(\widetilde{c}_4 + \frac{1}{4\,m}\Big)\Sigma_{ijk}^{(-)}\,\mathcal{T}_{ijk}^{(-)}\Big] \ , \qquad (2)$$

with spin and isospin operator structures defined, respectively, as $\Sigma_{lm} \equiv \widetilde{Z}_\pi(r_{lm})\,\boldsymbol{\sigma}_l \cdot \hat{\mathbf{r}}_{lm}$, where $\mathbf{r}_{lm} \equiv \mathbf{r}_l - \mathbf{r}_m$, and

$$\Sigma_{ijk}^{(\mp)} \equiv \Big[\widetilde{X}_{ij}\,,\,\widetilde{X}_{jk}\Big]_\mp \ , \quad \mathcal{T}_{ijk}^{(\mp)} \equiv [\boldsymbol{\tau}_i\cdot\boldsymbol{\tau}_j\,,\,\boldsymbol{\tau}_j\cdot\boldsymbol{\tau}_k]_\mp \ , \qquad (3)$$

$$\widetilde{X}_{ij} \equiv \widetilde{T}_\pi(r_{ij})\, S_{ij} + \widetilde{Y}_\pi(r_{ij})\, \boldsymbol{\sigma}_i \cdot \boldsymbol{\sigma}_j \ . \tag{4}$$

Here $[\dots,\dots]_\mp$ denote commutators ($-$) or anti-commutators ($+$), S_{ij} is the standard tensor operator, $\boldsymbol{\sigma}_i$ and $\boldsymbol{\tau}_i$ are Pauli spin and isospin matrices relative to nucleon i, and $\widetilde{Y}_\pi(r)$, $\widetilde{T}_\pi(r)$, and $\widetilde{Z}_\pi(r)$ are, respectively, standard Yukawa and tensor functions and combinations of these, regularized by the cutoff $C_{R_{\rm L}}(r)$ introduced in Ref. [37] (for convenience, they are listed in the online supplemental materials [46]). The LECs $\widetilde{c}_3$ and $\widetilde{c}_4$ are related to the corresponding c_3 and c_4 in $\mathcal{L}^{(2)}_{\pi N}$ via $\widetilde{c}_3 = c_3 - h_A^2/(9\, m_{\Delta N})$ and $\widetilde{c}_4 = c_4 + h_A^2/(18\, m_{\Delta N})$, where h_A and $m_{\Delta N}$ are, respectively, the N-to-Δ axial coupling constant and Δ-N mass difference. The values of these constants as well as the LECs c_1, c_3, and c_4, the (average) pion mass m_π and decay amplitude f_π, and (average) nucleon mass m and axial coupling constant g_A, are taken from Tables I and II of Ref. [37].

The CT term is parametrized as

$$V^{\rm CT}_{ijk} = \frac{g_A\, c_D}{96\,\pi}\, \frac{m_\pi^3}{\Lambda_\chi\, f_\pi^4}\, \boldsymbol{\tau}_i \cdot \boldsymbol{\tau}_k\, \widetilde{X}_{ik}\, \left[\, C_{R_{\rm S}}(r_{ij}) + C_{R_{\rm S}}(r_{jk})\,\right] + \frac{c_E}{\Lambda_\chi\, f_\pi^4}\, \boldsymbol{\tau}_i \cdot \boldsymbol{\tau}_k\, C_{R_{\rm S}}(r_{ij})\, C_{R_{\rm S}}(r_{jk}) \ , \tag{5}$$

where $C_{R_{\rm S}}(r)$ is the Gaussian cutoff introduced in Ref. [37] (it is also given in Ref. [46]), Λ_χ is the chiral-symmetry-breaking scale taken as $\Lambda_\chi = 1$ GeV, and the two (dimensionaless) LECs c_D and c_E are determined by simultaneously reproducing the experimental ^{3}H ground-state energy, $E_0(^3{\rm H})$, and the central value of the neutron-deuteron (nd) doublet scattering length, $^2a_{nd}$. These observables are calculated with hyperspherical-harmonics (HH) expansion methods (see Ref. [47] and references therein).

Due to the strong correlation between the observables $E_0(^3{\rm H})$ and $^2a_{nd}$ (Phillips line) and between $E_0(^3{\rm H})$ and $E_0(^4{\rm He})$ (Tjon line), an alternative way to determine c_D and c_E, as pointed out in Refs. [48, 49], would be to constrain these LECs by reproducing the tritium binding energy and Gamow-Teller matrix element contributing to its β-decay. Such a strategy was adopted in Refs. [50, 51] in relation to the (momentum-space) chiral interactions developed by Entem and Machleidt [18]. However, the problem with its implementation here is that the models of nuclear axial currents developed so far in Refs. [52, 53], do not include Δ intermediate states, in contrast to the present chiral interactions.

The c_D, c_E values for each NV2-I(a-b) and NV2-II(a-b) with the cutoff radii $(R_{\rm S}, R_{\rm L})$ in the Norfolk $3N$ interactions matching those of the corresponding NV2s to make the NV2+3 models are listed in Table I. We observe that models NV2-Ic and NV2-IIc are not considered any further in the present work, owing to the difficulty in the convergence of the HH expansion and the severe fermion-sign problem in the GFMC imaginary-time propagation with these interactions [36].

TABLE I. The (dimensionaless) values of c_D and c_E determined for the different NV2+3 chiral interactions having cutoff radii $(R_{\rm S}, R_{\rm L})$ equal to (0.8,1.2) fm for models Ia and IIa, and (0.7,1.0) fm for models Ib and IIb are shown along with the ^{3}H, ^{3}He, and ^{4}He ground-state energies (in MeV) and nd doublet scattering length (in fm), obtained in HH calculations without and with the inclusion of the three-body interactions; the experimental values are $E_0(^3{\rm H}) = -8.482$ MeV, $E_0(^3{\rm He}) = -7.718$ MeV, $E_0(^4{\rm He}) = -28.30$ MeV [54], and $^2a_{nd} = (0.645 \pm 0.010)$ fm [55]. The $E_0(^3{\rm H})$ and $^2a_{nd}$ (central value) are exactly reproduced when $3N$ interactions are included, and are not listed below in this case.

			w/o $3N$				with $3N$	
Model	c_D	c_E	$E_0(^3{\rm H})$	$E_0(^3{\rm He})$	$E_0(^4{\rm He})$	$^2a_{nd}$	$E_0(^3{\rm He})$	$E_0(^4{\rm He})$
Ia	3.666	–1.638	–7.825	–7.083	–25.15	1.085	–7.728	–28.31
Ib	–2.061	–0.982	–7.606	–6.878	–23.99	1.284	–7.730	–28.31
IIa	1.278	–1.029	–7.956	–7.206	–25.80	0.993	–7.723	–28.17
IIb	–4.480	–0.412	–7.874	–7.126	–25.31	1.073	–7.720	–28.17

In Table I we also report the nd scattering length and ground-state energies of ^{3}H, ^{3}He, and ^{4}He obtained without $3N$ interaction as well as those predicted for ^{3}He and ^{4}He when this interaction is included. Increasing the laboratory-energy range over which the NN interaction is fitted, from 0–125 MeV in class I to 0–200 MeV in class II, decreases the $A = 3$–4 ground-state energies calculated without the $3N$ interaction by as much as 1.3 MeV in ^{4}He with model b. However, when the $3N$ interaction is included, the effect is reversed and much reduced; in ^{4}He the increase amounts to 140 keV in going from model Ib to IIb. The dependence on the cutoff radii $(R_{\rm S}, R_{\rm L})$, *i.e.*, the difference between the rows Ia-Ib and IIa-IIb, is significant without the $3N$ interaction, but turns out to be negligible when it is retained, being in this case of the order of a few keV and hence comparable to the numerical

precision of the present HH methods. This tradeoff is of course achieved through the large variation of the LECs c_D and c_E; c_E is found to be natural for all models, while c_D only for models Ib and IIa. Lastly, in the online supplemental materials [46], we show that the NV2+3 chiral interactions developed here do not resolve the discrepancies between the calculated and measured polarization observables in low-energy *pd* elastic scattering, including the well-known "A_y puzzle" [56, 57].

Before presenting the GFMC predictions for the spectra of larger nuclei, it is worthwhile comparing the HH and GFMC results for the three- and four-nucleon bound states. The GFMC-calculated ground-state energies with model NV2+3-Ia are $E_0(^3\mathrm{H}) = -8.463(9)$, $E_0(^3\mathrm{He}) = -7.705(9)$, and $E_0(^4\mathrm{He}) = -28.24(3)$, where the Monte Carlo statistical errors are given in parentheses. The small differences ($\lesssim 0.5\%$) between the HH results listed in Table I and the GFMC ones are due in part to intrinsic numerical inaccuracies of these methods, and in part to the fact that the HH wave functions include small admixtures with total isospin $T = 3/2$ for $A = 3$ nuclei, and $T = 1$ and 2 for $A = 4$, beyond their corresponding dominant isospin components with $T = 1/2$ and $T = 0$. These admixtures are induced by ISB terms present in the NV2 interaction models, which are neglected in the present GFMC calculations.

The GFMC energy results calculated with the NV2+3-Ia model are shown in Fig. 2 for 37 different nuclear states in A=4–12 nuclei. They are compared to results from the older AV18+IL7 model [1] and experiment [54]. The agreement with experiment is impressive for both Hamiltonians, with absolute binding energies very close to experiment, and excited states reproducing the observed ordering and spacing, indicating reasonable one-body spin-orbit splittings. The rms energy deviation from experiment for these states is 0.72 MeV for NV2+3-Ia compared to 0.80 MeV for AV18+IL7 (note that ^{11}B has not been computed with AV18+IL7). The signed average deviations, +0.15 and −0.23 MeV respectively, are much smaller, indicating no systematic over- or under-binding of the Hamiltonians. For both Hamiltonians, the inclusion of the $3N$ interactions is in many cases necessary to get ground states that are correctly bound against breakup, *e.g.*, ^{6}He is not bound with just the NN interaction [36], but is in the current work. The lowest 3^+ and 1^+ states of ^{10}B are of particular interest. For both AV18 and NV2-Ia without $3N$ interactions, the 1^+ state is incorrectly predicted as the ground state (for NV2-Ia by 1.9 MeV) but including the $3N$ interactions gives the correct 3^+ ground state. However, it is important to emphasize that in the AV18+IL7 model the four parameters in the $3N$ interaction are fitted to the energies of many nuclear levels up to $A = 10$.

Twelve of the states shown are stable ground states, while another six are particle-stable low-lying excitations, *i.e.*, they decay only by electroweak processes. The remaining states are particle-unstable, *i.e.*, they can decay by nucleon or cluster emission, which is much more rapid than electroweak decay, but about half of these have narrow decay widths ≤ 100 keV. Because GFMC does not involve any expansion in basis functions, it correctly includes effects of the continuum. If the energy propagation is continued to large enough imaginary time, the wave function will evolve to separated clusters and the energy to the sum of the energies of those clusters. For the physically narrow states, the GFMC constrained-path propagation starting from a confined variational trial function reaches a stable energy without any noticeable decay over the finite τ used in the present calculations. For physically very wide states (> 1 MeV), *e.g.*, the first 2^+ and 4^+ states in ^{8}Be, the calculations show a smooth energy decline beyond $\tau \sim 0.1$ MeV^{-1} [58], while the rms radius shows a smooth growth, indicative that the propagation is disassembling the system into its component parts. In these few cases the energy of the state is estimated from the value at the beginning of the smooth energy decline. Additional particle-stable isobaric analog states, *e.g.*, in ^{8}B and ^{9,10}C, have been calculated in GFMC, but are not shown.

A VMC survey of more than 60 additional states has also been made, including higher excited states, more isobaric analog states, *e.g.*, in ^{7}Be, and various particle-unstable nuclei like ^{7}He, ^{8}C, and ^{9}B. While the most important test of a Hamiltonian is the ability to reproduce known states, it is also important *not* to predict states in places where they are not observed, *e.g.*, predicting a particle-stable ^{10}He ground state would be a failure of the model. The VMC survey has found no such problems for either the NV2+3-Ia or AV18+IL7 models.

The very satisfactory agreement between the predicted and observed spectra validates the present formulation of the basic model in terms of NN and $3N$ chiral interactions, constrained by data in the few-nucleon systems only. Of course, one should not dismiss the earlier success of the AV18/IL7 realistic interactions, even though the agreement in that case was obtained by relying on experimental data beyond $A = 3$ in order to constrain the $3N$ interaction. If anything, the overall success of the chiral and realistic formulations shows that Hamiltonians containing two very different models of the NN force, both of which provide good fits to NN data, and $3N$ forces containing just a small number of parameters fitted to a few data, can give very similar descriptions of light-nuclei spectra. This gives us confidence in predictions made in the framework of the basic model of nuclear theory.

Key to this significant advance is our group's ability to reliably solve the nuclear many-body problem for bound states of up to $A = 12$ nuclei with QMC methods, and for the three- and four-nucleon bound and scattering states with HH methods. This capability, especially for QMC, is driven by ever expanding computational resources and by continuing improvements in algorithms. In particu-

lar, the development of specific libraries operating under MPI [59]—the Asynchronous Dynamic Load Balancing (ADLB) library and Distributed MEMory (DMEM) library—have allowed us to fully exploit the massively parallel Theta supercomputer (3,624 Intel Knight's Landing nodes with 64 cpus/node) of the Argonne Leadership Computing Facility. Even under these favorable conditions, however, the final ^{12}C ground-state calculation still consumed 650,000 cpu-hours.

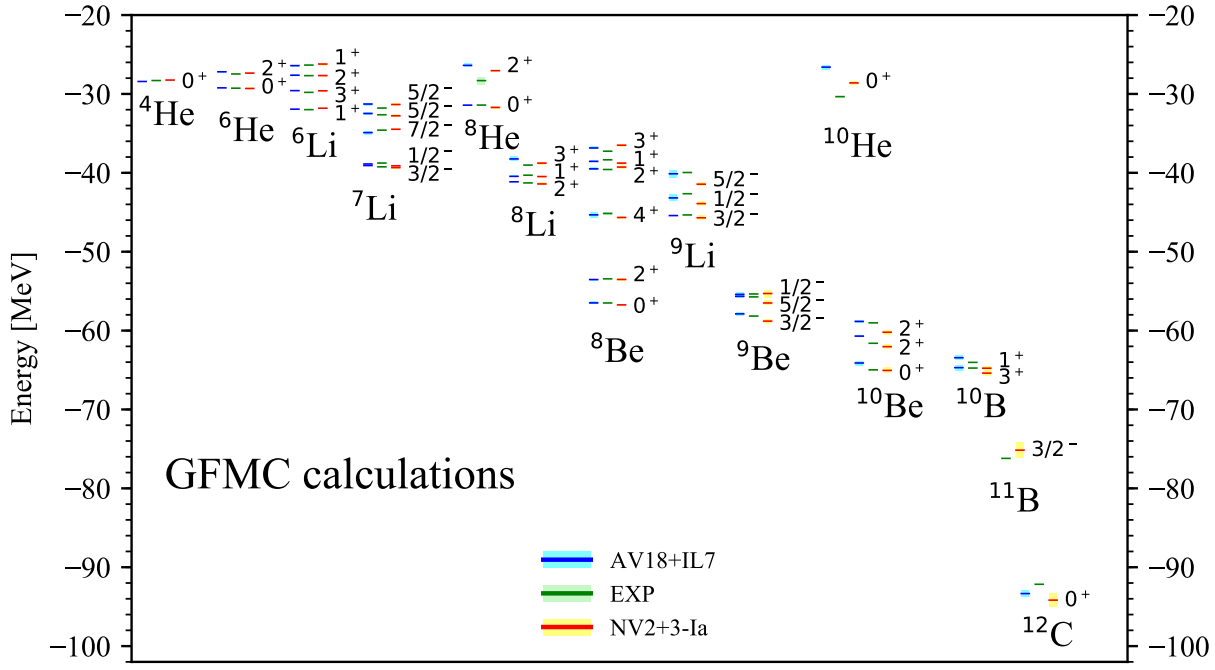

FIG. 2. The energy spectra of $A = 4$–12 nuclei obtained with the NV2+3-Ia chiral interactions are compared to experimental data [54]. Also shown are results obtained with the phenomenological AV18+IL7 interactions [1].

Future work will investigate the other chiral Hamiltonian models developed here, in particular their impact on nuclear spectra, as well as refinements in the $3N$ interaction obtained by retaining subleading terms [23, 60] and by constraining them via fits to either nuclear spectra or $3N$ scattering observables.

The work of M.P., A.L., E.L., S.C.P., and R.B.W has been supported by the NUclear Computational Low-Energy Initiative (NUCLEI) SciDAC project. This research is further supported by the U.S. Department of Energy, Office of Science, Office of Nuclear Physics, under contracts DE-AC02-06CH11357 (M.P., A.L., S.C.P., and R.B.W.) and DE-AC05-06OR23177 (R.S.). It used computational resources provided by Argonne's Laboratory Computing Resource Center, by the Argonne Leadership Computing Facility, which is a DOE Office of Science User Facility supported under Contract DE-AC02-06CH11357 (via a Theta Early Science grant), and by the National Energy Research Scientific Computing Center (NERSC).

[1] J. Carlson *et al.*, *Rev. Mod. Phys.* **87**, 1067 (2015).
[2] H. Yukawa, *Proc. Phys. Math. Soc. Japan* **17**, 48 (1935).
[3] V.G.J. Stoks, R.A.M. Klomp, C.P.F. Terheggen, and J.J.

de Swart, *Phys. Rev. C* **49**, 2950 (1994).
[4] R.B. Wiringa, V.G.J. Stoks, and R. Schiavilla, *Phys. Rev. C* **51**, 38 (1995).
[5] R. Machleidt, *Phys. Rev. C* **63**, 024001 (2001).
[6] V.G.J. Stoks, R.A.M. Klomp, M.C.M. Rentmeester, and J.J. de Swart, *Phys. Rev. C* **48**, 792 (1993).
[7] J.L. Friar, B.F. Gibson, and G.L. Payne, *Annu. Rev. Nucl. Part. Sci.* **34**, 403 (1984).
[8] B.S. Pudliner, V.R. Pandharipande, J. Carlson, S.C. Pieper, and R.B. Wiringa, *Phys. Rev. C* **56**, 1720 (1997).
[9] P. Navrátil, J.P. Vary, and B.R. Barrett, *Phys. Rev. C* **62**, 054311 (2000).
[10] S.C. Pieper, V.R. Pandharipande, R.B. Wiringa, and J. Carlson, *Phys. Rev. C* **64**, 014001 (2001).
[11] J. Fujita and H. Miyazawa, *Prog. Theor. Phys.* **17**, 360 (1957).
[12] S.C. Pieper, *AIP Conf. Proc.* **1011**, 143 (2008).
[13] S. Weinberg, *Phys. Lett. B* **251**, 288 (1990).
[14] S. Weinberg, *Nucl. Phys. B* **363**, 3 (1991).
[15] S. Weinberg, *Phys. Lett. B* **295**, 114 (1992).
[16] C. Ordonez, L. Ray, and U. van Kolck, *Phys. Rev. C* **53**, 2086 (1996).
[17] E. Epelbaum, W. Glöckle, and U.-G. Meissner, *Nucl. Phys. A* **637**, 107 (1998).
[18] D.R. Entem and R. Machleidt, *Phys. Rev. C* **68**, 041001 (2003).
[19] R. Machleidt and D.R. Entem, *Phys. Rep.* **503**, 1 (2011).
[20] U. van Kolck, *Phys. Rev. C* **49**, 2932 (1994).
[21] E. Epelbaum *et al.*, *Phys. Rev. C* **66**, 064001 (2002).
[22] V. Bernard, E. Epelbaum, H. Krebs, and U.-G. Meissner, *Phys. Rev. C* **84**, 054001 (2011).
[23] L. Girlanda, A. Kievsky, and M. Viviani, *Phys. Rev. C* **84**, 014001 (2011).
[24] H. Krebs, A. Gasparyan, and E. Epelbaum, *Phys. Rev. C* **85**, 054006 (2012).
[25] A. Ekström *et al.*, *Phys. Rev. Lett.* **110**, 192502 (2013).
[26] A. Ekström *et al.*, *Phys. Rev. C* **91**, 051301(R) (2015).
[27] E. Epelbaum, H. Krebs, and U.-G. Meißner, *Eur. Phys. J. A* **51**, 53 (2015).
[28] P. Navrátil, *Few Body Syst.* **41**, 117 (2007).
[29] I. Tews, S. Gandolfi, A. Gezerlis, and A. Schwenk, Phys. Rev. C **93**, 024305 (2016).
[30] A. Ekström *et al.*, arXiv:1707.09028.
[31] J.L. Friar and U. van Kolck, *Phys. Rev. C* **60**, 034006 (1999).
[32] J.L. Friar, U. van Kolck, M.C.M. Rentmeester, and R.G.E. Timmermans, *Phys. Rev. C* **70**, 044001 (2004).
[33] J.L. Friar, G.L. Payne, and U. van Kolck, *Phys. Rev. C* **71**, 024003 (2005).
[34] A. Gezerlis *et al.*, *Phys. Rev. Lett.* **111** (3), 032501 (2013).
[35] A. Gezerlis *et al.*, *Phys. Rev. C* **90**, 054323 (2014).
[36] M. Piarulli *et al.*, *Phys. Rev. C* **94**, 054007 (2016).
[37] M. Piarulli *et al.*, *Phys. Rev. C* **91**, 024003 (2015).
[38] D.B. Kaplan, M.J. Savage, and M.B. Wise, *Phys. Lett.* B **424**, 390 (1998); *Nucl. Phys. B* **534**, 329 (1998).
[39] A. Nogga, R.G.E. Timmermans, and U. van Kolck, *Phys. Rev. C* **72**, 054006 (2005).
[40] M.C. Birse, *Phys. Rev. C* **74**, 014003 (2006).
[41] M.P. Valderrama and D.R. Phillips, *Phys. Rev. Lett.* **114**, 082502 (2015).
[42] R.N. Pérez, J.E. Amaro, and E.R. Arriola, *Phys. Rev. C* **88**, 024002 (2013); *ibidem*, 069902(E) (2013).
[43] J.E. Lynn *et al.*, *Phys. Rev. Lett.* **116**, 062501 (2016).
[44] J.E. Lynn *et al.*, arXiv:1706.07668
[45] N. Fettes, U.-G. Meissner, M. Mojzis, and S. Steininger, *Ann. Phys.* **283**, 273 (2000); *ibidem* **288**, 249 (E) (2001).
[46] Online supplemental material.
[47] A. Kievsky, S. Rosati, M. Viviani, L.E. Marcucci, and L. Girlanda, *J. Phys. G: Nucl. Part. Phys.* **35**, 063101 (2008).
[48] A. Gårdestig and D. R. Phillips, Phys. Rev. Lett. **96**, 232301 (2006).
[49] D. Gazit, S. Quaglioni, and P. Navrátil, Phys. Rev. Lett. **103**, 102502 (2009).
[50] L.E. Marcucci, A. Kievsky, S. Rosati, R. Schiavilla, and M. Viviani, Phys. Rev. Lett. **108**, 052502 (2012).
[51] A. Baroni, L. Girlanda, A. Kievsky, L.E. Marcucci, R. Schiavilla, and M. Viviani, *Phys. Rev. C* **94**, 024003 (2016); Erratum Phys. Rev. C **95**, 059902 (2017).
[52] A. Baroni, L. Girlanda, S. Pastore, R. Schiavilla, and M. Viviani, *Phys. Rev. C* **93**, 015501 (2016).
[53] H. Krebs, E. Epelbaum, and U.-G. Meiner, *Ann. Phys.* **378**, 317 (2017).
[54] G. Audi, A.H. Wapstra, and C. Thibault, *Nucl. Phys. A* **729**, 337 (2003).
[55] K. Schoen *et al.*, *Phys. Rev. C* **67**, 044005 (2003).
[56] W. Glöckle, H. Witala, D. Hüber, H. Kamada, and J. Golak, *Phys. Rep.* **274**, 107 (1996).
[57] S. Shimizu *et al.*, Phys. Rev. C **52**, 1193 (1995).
[58] S. Pastore, R.B. Wiringa, S.C. Pieper, and R. Schiavilla, *Phys. Rev. C* **90**, 024321 (2014).
[59] E. Lusk, R. Butler, and S.C. Pieper, *The International Journal of High Performance Computing Applications* DOI: 10.1177-1094342017703448 (2017).
[60] J. Golak *et al.*, Eur. Phys. J. A **50**, 177 (2014).